Biogeosciences Discuss., 11, 5179–5214, 2014
www.biogeosciences-discuss.net/11/5179/2014/
doi:10.5194/bgd-11-5179-2014

Biogeosciences Discussions
Open Access

Flexible C : N ratio enhances metabolism of large phytoplankton when resource supply is intermittent

D. Talmy[1,2,4], J. Blackford[2], N. J. Hardman-Mountford[3], L. Polimene[2], M. J. Follows[4], and R. J. Geider[1]

[1]School of Biological Sciences, University of Essex, Wivenhoe Park, Colchester, UK
[2]Plymouth Marine Laboratory, Prospect Place, The Hoe, Plymouth, Devon, UK
[3]Commonwealth Scientific and Industrial Research Organization, Marine and Atmospheric Research, Centre for Environment and Life Sciences, Floreat, Australia
[4]Department of Earth, Atmosphere and Planetary Sciences, Massachusetts Institute of Technology, Cambridge, Massachusetts, USA

Received: 21 March 2014 – Accepted: 25 March 2014 – Published: 1 April 2014

Correspondence to: D. Talmy (dtalmy@mit.edu)

Published by Copernicus Publications on behalf of the European Geosciences Union.

Abstract

Phytoplankton cell size influences particle sinking rate, food web interactions and biogeographical distributions. We present a model in which the uptake, storage and assimilation of nitrogen and carbon are explicitly resolved in different sized phytoplankton cells. In the model, metabolism and cellular C : N ratio are influenced by accumulation of carbon polymers such as carbohydrate and lipid, which is greatest when cells are nutrient starved, or exposed to high light. Allometric relations and empirical datasets are used to constrain the range of possible C : N, and indicate larger cells can accumulate significantly more carbon storage compounds than smaller cells. When forced with extended periods of darkness combined with brief exposure to saturating irradiance, the model predicts organisms large enough to accumulate significant carbon reserves may on average synthesize protein and other functional apparatus up to five times faster than smaller organisms. The advantage of storage in terms of average daily protein synthesis rate is greatest when modeled organisms were previously nutrient starved, and carbon storage reservoirs saturated. Small organisms may therefore be at a disadvantage in terms of average daily growth rate in environments that involve prolonged periods of darkness and intermittent nutrient limitation. We suggest this mechanism is a significant constraint on phytoplankton C : N variability and cell size distribution in different oceanic regimes.

1 Introduction

Through its influence on resource acquisition (Pasciak and Gavis, 1974), growth (Tang, 1995) and food-web interactions (Armstrong, 1994), organism size is thought to play a major role structuring marine plankton communities (Chisholm, 1992). A few primary productivity (PP) algorithms (Kameda and Ishizaka, 2005; Hirata et al., 2008; Uitz et al., 2008; Brewin et al., 2010) and several other oceanic ecosystem models (e.g. Blackford et al., 2004; Le Quere et al., 2005) resolve phytoplankton traits as a function of cell

BGD
11, 5179–5214, 2014

size. Hence, there is a need to understand how metabolism and photophysiological traits scale with organism size.

Due to their relatively high surface area to volume ratio, small cells are thought to be superior competitors for nutrients in oligotrophic environments (Chisholm, 1992; Clark et al., 2013). Furthermore, pigment packaging in large organisms can lead to a reduction in light absorption per unit chlorophyll (Morel and Bricaud, 1981), again conferring an advantage to smaller organisms. The prevalence of large organisms in eutrophic ecosystems is usually explained by enhanced resilience to predation (e.g. Ward et al., 2012), and greater nutrient storage capacity. For example, using a Droop model of algal growth in a model chemostat, Verdy et al. (2009) showed the positive influence on growth of a large internal storage reservoir. Furthermore, Grover (1991a, 1991b, 2011) and Tozzi et al. (2004) have demonstrated the benefit of enhanced storage capacity in environments with infrequent nutrient pulses. In general, studies that have assessed the ecological advantage of storage have tended to focus on the benefits associated with an enhanced capacity to store nutrients such as nitrogen, phosphorus and iron. Yet, at high lattitude where there is low average surface irradiance and relatively deep mixing (Fig. 1), phytoplankton growth is likely to be light limited.

With sufficiently high irradiance, many phytoplankton species can accumulate large stores of carbohydrate and lipid (Granum et al., 2002). In darkness, these reserves may be drawn upon both as a source of energy to fuel metabolism, and as a source of organic carbon to incorporate into proteins and cell structure. Vertical mixing and the diurnal cycle cause phytoplankton to regularly experience prolonged exposure to chronically low irradiance or darkness (Dubinsky and Schofield, 2010). Therefore, the ability to store carbon may be critical to survival, and may also be a vital ecological strategy when growth maximization determines fitness.

We use an empirically constrained phytoplankton growth model to understand how storage capacity influences growth in environments with intermittent nitrogen supply and photon flux density (PFD). The model uses published allometric relations to constrain the capacity for storage. We begin with an overview of the mathematical relations

BGD
11, 5179–5214, 2014

used to constrain growth and go on to describe the theory and experimental datasets used to constrain model parameters. We demonstrate the model can be constrained to fit observations of organisms in balanced growth. Finally, we report the influence of cell size and carbon storage on the ability of cells to grow when PFD and nitrogen supply are intermittent, and discuss potential implications of our results for the distribution and biogeochemistry of marine phytoplankton.

2 Methods

2.1 Model overview

The model (Fig. 2) is designed to mechanistically capture intracellular dynamics of nitrogen and carbon using simple, previously established mathematical relations. Photosynthesis and uptake are responsible for additions to internal storage reservoirs of carbon and nitrogen, respectively. Photosynthesis is parameterized with a photoacclimation model that allows allocation to light harvesting proteins to vary dynamically in response to ambient irradiance conditions. Nitrogen is assumed to enter a subcellular reserve pool as a Michaelis–Menten function of the surrounding subsrate concentration. Reserve nitrogen and carbon are converted into proteins via the cell's biosynthetic apparatus. Protein synthesis only ceases when internal reserves of nitrogen or carbon are depleted, and reserves only accumulate when either photosynthesis or uptake exceed protein synthesis. Thus, variations in cellular C : N ratio arise when there is an imbalance between photosynthesis, nutrient uptake and the synthesis of functional apparatus.

Allometric relations that constrain nutrient uptake, storage capacity and light absorption were used to parameterize the model. Remaining parameters were tuned to empirical datasets for organisms spanning an appropriate size range. This section contains a detailed overview of the model equations, and a description of the allometric relations and empirical datasets used to constrain parameter values.

BGD
11, 5179–5214, 2014

2.2 Model equations

The model explicitly resolves intracellular reserve pools of compounds that contain either nitrogen or carbon, but not both (Fig. 2 has a model schematic, and Table 1 has all parameter definitions and units). The reserve nitrogen pool is assumed to consist only of NO_3^-. The reserve carbon pool may contain any monosaccharides, non-structural polysaccharides and non-structural lipids. These reserve pools serve as input reservoirs of nitrogen and carbon to a mixed pool. The mixed pool contains all "functional" cellular apparatus that regulate metabolism. It may include, but is not limited to, proteins, pigments, nucleic acids, amino acids and structural lipids. The following four equations parameterize growth in terms of these intracellular pools:

$$\frac{1}{N_F}\frac{dN_R}{dt} = V_n - \mu \quad (1)$$

$$\frac{1}{N_F}\frac{dC_R}{dt} = P_n - \left(\frac{1}{\eta} + \zeta\right)\mu - \frac{R_0}{\eta} \quad (2)$$

$$\frac{1}{N_F}\frac{dN_F}{dt} = \mu - R_0 \quad (3)$$

$$\frac{1}{N_F}\frac{dN_{LH}}{dt} = \rho_{LH}\mu - F_{LH}R_0 \quad (4)$$

The reserve nitrogen and carbon pools are denoted N_R and C_R respectively. Although here N_F denotes the nitrogen content of the functional pool, we impose a fixed stoichiometry on this pool, so that functional nitrogen and carbon may be related with $N_F = \eta C_F$ where η is the imposed N : C ratio in $gN(gC)^{-1}$. The light harvesting apparatus, denoted here N_{LH}, are part of the functional pool, but are nonetheless modeled with a separate state variable (Eq. 4). Synthesis of light harvesting apparatus is regulated with the function ρ_{LH} (see below), to simulate variations in nitrogen allocation that occur during photoacclimation (McKew et al., 2013). Losses associated with the carbon and energy costs of basal metabolism are encapsulated with the fixed parameter

BGD
11, 5179–5214, 2014

R_0. Each term on the right hand side of Eqs. (1) to (4) is now described in detail. Note that all parameter definitions and units may be found in Table 1.

Inorganic nitrogen (denoted here S, for "substrate") first enters the reserve pool via a Michaelis–Menten style parameterization of uptake:

$$V_n = V_m \frac{S}{S + K_S} \tag{5}$$

In Eq. (5), V_m and K_S are the maximum uptake and half saturation coefficients of the Michaelis–Menten relationship. The maximum rate of nitrogen uptake is a linearly decreasing function of the internal nitrogen reserve (e.g. Thingstad, 1987):

$$V_m = \left(1 - \frac{N_R}{N_R^{max}}\right) V_{max} \tag{6}$$

Carbon fixed via photosynthesis enters the reserve pool via the following, photosynthesis–irradiance relationship:

$$P_n = P_m \left(1 - \exp\left(-\frac{\alpha F_{LH} E}{P_m}\right)\right) \tag{7}$$

where the maximum rate of photosynthesis is a linearly decreasing function of the internal carbon reserve (see Fig. 3):

$$P_m = \left(1 - \frac{C_R}{C_R^{max}}\right) P_{max} \tag{8}$$

In Eq. (7), the initial slope of the photosynthesis-irradiance curve is dependent on the fraction of intracellular nitrogen allocated to light harvesting: $F_{LH} = N_{LH}/N_F$. Because both N_{LH} and N_F are state variables, F_{LH} is a dynamic representation of the cell's

BGD
11, 5179–5214, 2014

nitrogen allocation to light harvesting. Here we constrain this fraction with the regulatory function ρ_{LH}, analagous to the approach of Geider et al. (1997, 1998):

$$\rho_{LH} = F_{LH}^{max} \max\left\{\frac{1}{1 + F_{LH}^{G} E}, \frac{F_{LH}^{min}}{F_{LH}^{max}}\right\} \quad (9)$$

With Eq. (9), the proportion of newly fixed nitrogen allocated to the synthesis of light harvesting pigments is a decreasing function of the ambient PFD (see Fig. 4), which enables the investment in light harvesting apparatus as a function of growth irradiance to be constrained empirically. Thus, the trade-off between nitrogen allocation to light harvesting and other apparatus such as the photoprotective machinery (Armstrong, 2006; McKew et al., 2013) is not considered in this work.

The flow of resources from reserve pools to the functional pool is parameterized as the minimum between two, Michaelis–Menten style functions of the internal reserves:

$$\mu = \min\left\{\frac{N_R/N_F}{K_N + N_R/N_F}, \frac{C_R/C_F}{K_C + C_R/C_F}\right\} \mu'_{max} \quad (10)$$

Where the reserve concentration is normalized by the concentration of the functional pool; an appropriate constraint for situations in which reserves are not significantly more abundant than enzymes involved in metabolism (Borghans et al., 1996).

There is evidence that dark N assimilation proceeds at a lower rate than in the light (DiTullio and Laws, 1986; Probyn et al., 1996; Ross and Geider, 2009). Reductions in dark N assimilation are assumed to influence μ in the following way:

$$\mu'_{max} = \begin{cases} \mu_{max} & \text{if } E > 0 \\ a_N \mu_{max} & \text{otherwise.} \end{cases} \quad (11)$$

Equation (10) simulates internal conversion of C and N into protein and other functional apparatus. When the flow of carbon and nitrogen into the reserve pool from the

BGD
11, 5179–5214, 2014

surrounding medium is equal to the subsequent rate of removal into the functional pool, the cell is said to be in balanced growth. All datasets used for comparison were of organisms in balanced growth, and so Eq. (10) was treated as the effective growth rate.

When either ambient photons or N supply are limiting, cells are able to draw on at least one internal resource to maintain active metabolism. In such conditions, Eq. (11) is only comparable to the specific growth rate of the non-limiting abiotic resource. It is not directly comparable to the net accumulation of the limiting resource, which is strictly less than μ.

2.3 Allometry

2.3.1 The package effect

Let a^*_{ph} denote the theoretical, spectrally integrated absorption cross-section of a unit of nitrogen contained in the light harvesting apparatus (with units $\mathrm{m}^2\,(\mathrm{g\,N})^{-1}$), assuming that the light harvesting apparatus was in no way influenced by pigment packaging. In other words, it is the absorption cross-section of pigment associated with each unit of nitrogen in the light harvesting apparatus in solution. Furthermore, let c_i denote the concentration of cellular nitrogen associated with the light harvesting apparatus (units $\mathrm{g\,N\,m}^{-3}$). If η is the N : C ratio of the main functional apparatus and V is the cell volume, then with knowledge of the cellular carbon quota and the fraction of cellular nitrogen allocated to light harvesting (F_{LH}), c_i may be calculated with:

$$c_i = \left(\frac{F_{\mathrm{LH}} Q^{\mathrm{C}}_{\mathrm{max}} \eta}{V} \right) \tag{12}$$

Note that, because we do not follow individual cell quotas explicitly, we assume a fixed cell carbon content, $Q^{\mathrm{C}}_{\mathrm{max}}$. Following Morel and Bricaud (1981), the actual absorption of pigment packaged within a cell of diameter d (with units m) with c_i grams

BGD
11, 5179–5214, 2014

of nitrogen contained in chlorophyll (units $\mathrm{g\,N\,m^{-3}}$) may be calculated with:

$$a_{\mathrm{ph}} = \frac{3}{2} a^{*}_{\mathrm{ph}} \frac{Q(\rho)}{\rho} \tag{13}$$

where

$$Q(\rho) = 1 + \frac{2e^{-\rho}}{\rho} + \frac{2(e^{-\rho} - 1)}{\rho^2} \tag{14}$$

and

$$\rho = a^{*}_{\mathrm{ph}} c_i d \tag{15}$$

The initial slope of the photosynthesis-irradiance response curve may then be constrained as a function of cell size, with knowledge of the maximum quantum efficiency of photosynthesis, ϕ_{m}:

$$\alpha = a_{\mathrm{ph}} \phi_{\mathrm{m}} \gamma \tag{16}$$

Empirical allometric relations suggest the initial slope of the growth-irradiance curve may be negatively correlated with cell size across taxa (Edwards et al., 2014). Yet, there is considerable scatter in the data, probably due in part to different pigment compositions, non-spherical cell shapes, and non-homogeneous intracellular pigment distributions. We include γ in the above relation as a tuning parameter to account for these differences when fitting the model to data of different taxa.

2.3.2 Nitrogen storage

Cellular nitrogen quotas are known to change considerably as a function of the external substrate concentration to which cells are acclimated (Droop, 1973; Caperon and Meyer, 1972). The difference in cell quota that occurs under different growth conditions

BGD
11, 5179–5214, 2014

is thought to increase as a function of cell size, when maximal nitrogen quotas scale faster than minimal nitrogen quotas (Verdy et al., 2009). However, changes in nitrogen quota are usually accounted for primarily by changes in cellular protein content in different growth conditions (Dortch et al., 1984). Thus, changes in the total nitrogen quota as a function of cell size cannot be used directly to constrain the size of our nitrogen reserve pool, which may contain only inorganic forms of N.

In different species, inorganic nitrogen may contribute anywhere between 0 (Dortch et al., 1984) and ∼ 40 % (Lourenço et al., 1998) of total cellular nitrogen. We do not know of any previously reported studies of the size dependence of stored, inorganic nitrogen. We therefore assumed a maximum capacity for nitrogen storage that is invariant of cell size, such that:

$$N_{\mathrm{R}}^{\mathrm{max}} = f_{\mathrm{stor}} N_{\mathrm{F}} \tag{17}$$

Where f_{stor} is the maximum capacity for storage as a fraction of the total functional nitrogen concentration (see Table 1). We acknowledge this treatment may overlook a reduced capacity to store nitrogen in some very small prokaryotes.

2.3.3 Carbon storage

To the best of our knowledge, there are insufficient measurements of carbon storage quotas to directly infer allometric relations. We therefore parameterized the maximum capacity for carbon storage in the following way. Carbon contained in the functional pool (that includes pigments, nucleic acid, etc.) is expected to reach a minimum when cells are nutrient starved (Dortch et al., 1984). After Mei et al. (2011), the minimal carbon quota associated with the functional apparatus is (in mmol C cell^{-1}) (see also, Shuter, 1978):

$$Q_{\mathrm{F,min}}^{\mathrm{C}} = 9.9 \times 10^{-12} V^{0.72} \tag{18}$$

We assume that whole cell maximal carbon quotas ($Q_{\mathrm{max}}^{\mathrm{C}}$) are associated with cells grown under nutrient replete conditions, and scale as a power law function of cell vol-

BGD
11, 5179–5214, 2014

ume (Menden-Deuer and Lessard, 2000):

$$Q^{C}_{max} = 18 \times 10^{-12} V^{0.9} \quad (19)$$

Under nutrient limitation, cells divert fixed carbon away from biosynthesis of functional components, toward synthesis of reserve polymers (Rodolfi et al., 2009). Thus, we assume that differences in the functional carbon cell quota under nutrient limitation, and the maximum carbon quota under nutrient replete conditions, may be used to approximate the maximum potential capacity for carbon storage:

$$C^{max}_{R} = \left(\frac{Q^{C}_{max}}{Q^{C}_{F,min}} - 1 \right) C_{F} \quad (20)$$

The exponent in Eq. (19) is larger than the exponent in Eq. (18), so the capacity for carbon storage is expected to increase as a function of cell volume.

2.4 Model parameterization and experimental setup

The parameters in Table 4 were tuned to enable model predictions of growth, Chl : C and C : N to agree with measurements of several species of phytoplankton cultured in photon flux density (PFD) and nitrogen limiting conditions. In order to test the influence of storage capacity in a range of cell sizes, organisms selected include low light adapted *Prochlorococcus marinus* SS120 (Moore et al., 1995), high light adapted *P. marinus* (MED4) (Bertilsson et al., 2003), *Synechococcus* WH8012 and WH8103 (Moore et al., 1995), the freshwater strain *Synechococcus linearis* (Healey, 1985) and the diatom *Skeletonema costatum* (Sakshaug et al., 1989). All measurements are of organisms in balanced growth.

Most of the remaining model parameters were taken from allometry (Table 3). The carbon cost of nitrogen assimilation (ζ) and the quantum efficiency of photosynthesis (ϕ_m), were assumed based on previously established theoretical considerations (see

BGD
11, 5179–5214, 2014

Table 1). The reduction in dark N assimilation was constrained with data from DiTullio and Laws (1986) (see Table 2).

The influence of storage on growth rate is expected to be most evident when organisms transition between saturating resource supply, and resource limitation. The following experimental procedure was used to test the influence of intermittent nitrogen and photon supply on organism growth rates. First, as a reference, the growth rate was determined for model organisms exposed to a range of constant PFD and nitrogen supply rates. Then, to understand the influence of intermittent PFD and nitrogen supply on organism growth rates, modeled organisms were exposed to an intermittent PFD with constant nitrogen supply, and constant PFD with intermittent nitrogen supply. In all cases, nitrogen and PFD were switched between saturating availability, and complete scarcity. The period within which resources were abundant was varied within the range [0.01, 1.0] as a fraction of day length. Finally, because phytoplankton accumulate significantly more carbon reserves when subjected to nitrogen limitation, cells were acclimated to low nitrogen concentration before being subjected to intermittent PFD.

3 Results

3.1 Model-data comparisons

When cultured in nutrient replete conditions, the growth rates of *Prochlorococcus marinus* SS120, *Synechococcus* WH8103 and *Skeletonema costatum* (abbreviated SS120, WH8103 and *S. costatum*, respectively) all increase as a function of ambient PFD, eventually reaching a maximum at high PFD (Fig. 5). Furthermore, Chl : C declined with increasing growth irradiance in all three organisms. When the parameters in Table 4 were tuned to match experimental observations, the model is able to capture the observed dependence of growth rate and Chl : C on PFD for *Prochlorococcus* SS120, *Synechococcus* WH8103 and *S. costatum* (Fig. 5).

BGD
11, 5179–5214, 2014

Under nitrogen limitation, carbon fixed via photosynthesis is diverted away from protein synthesis, toward synthesis of carbohydrates and lipids (Rodolfi et al., 2009). Thus, when grown under nitrogen limitation, phytoplankton cultures tend to show increases in cellular C : N at low growth rates (Fig. 6). The model is able to replicate the dependence of C : N ratio on nitrogen limited growth rate for all species in Figs. 6 and 7.

The allometric relations for carbon storage quota suggest large phytoplankton cells are able to accumulate significantly more carbon reserves than small cells (Table 3). Thus, model predictions suggest large cells that accumulate relatively more storage lipid and carbohydrate should reach higher nitrogen limited C : N ratios. Model predictions of the size dependence of C : N ratio are supported by data corresponding to *P. marinus* (MED4), *Synechococcus* WH8103 and WH8103, *S. linearis* and *S. costatum* (Fig. 6).

3.2 Growth in a constant environment

Due to reduced package effects, and their high surface area to volume ratio, small cells are expected to have higher average growth rates than large cells when either PFD or nitrogen supply are limiting. In fact, when interspecific differences in the initial slope of the *P–E* curve are assumed to arise solely from size related pigment packaging, the model underpredicts observed growth rates of *S. costatum* (Fig. 5c), which suggests this diatom may only partially be influenced by pigment packaging. The advantage of small cell size is nonetheless evident at low nitrogen supply rates, even when the model is parameterized for *S. costatum* with a maximum growth rate approximately double that of *P. marinus* (SS120) (Figs. 5 and 9a). With sufficiently high PFD and nitrogen supply, *S. costatum* reaches its maximum growth rate, and any advantage of small cell size disappears (Fig. 9a).

BGD
11, 5179–5214, 2014

3.3 Intermittence experiments

The model predicts organisms with sufficiently large capacity for storage are able to accumulate carbon reserves under saturating PFD, which may subsequently be used to fuel growth in the dark (Fig. 8). Accumulation and subsequent mobilization of carbon reserves leads to fluctuations in the C : N ratio (Fig. 8a). Even when forced with intermittent PFD, the model predicts relatively invariant C : N ratio of small cells with limited capacity for carbon storage (Fig. 8a). Due to this inability to accumulate reserve carbon, the model predicts very small cells may be unable to maintain growth in the dark. Thus, model predictions suggest the ability to store carbon may confer an advantage to larger organisms under exposure to intermittent PFD (Fig. 8).

When forced with intermittent PFD, the model predicts *S. costatum* may on average grow more than twice as fast as *P. marinus* (SS120), even when the average daily PFD is extremely low (Fig. 9b). The benefit of small cell size nonetheless persists at very low nitrogen supply rate, even when the model is forced with intermittent PFD (Fig. 9b).

The model predicts *P. marinus* (SS120) should still grow faster than *S. costatum* at low average nitrogen supply rate, even when forced with intermittent nitrogen supply (Fig. 9c). Indeed, because the capacity for inorganic nitrogen storage is relatively low and invariant with cell size, there is almost no discernible influence of intermittent nitrogen pulses on the modeled balance between *S. costatum* and SS120 growth rates (Fig. 9c).

Phytoplankton carbon storage is expected to reach a maximum when organisms are nutrient starved (Rodolfi et al., 2009). Thus, one might expect the influence of variable PFD to change depending on phytoplankton nutrient status. Indeed, the modeled benefit of carbon storage in environments with intermittent PFD is greater in experiments that involved prior acclimation to low nitrogen supply rate, by comparison to experiments that involved prior acclimation to high nitrogen supply rate (Fig. 9b and d).

BGD
11, 5179–5214, 2014

4 Discussion

We used a model to understand how energy stored in carbohydrate and lipid influences phytoplankton growth rate in environments with ephemeral PFD. The model was parameterized in part using allometric relationships for carbon storage quotas and nutrient uptake rates (Table 3), and in part by fitting to experimental datasets (Table 4 and Fig. 5). This empirical parameterization led to the model prediction that the very smallest phytoplankton cells should have a low capacity to store carbon, which is associated with relatively inflexible C : N ratios (Fig. 8). Our model suggests that an inability to store carbon reduces the capacity for cells to synthesize functional biomass during darkness. In contrast, phytoplankton cells with the ability to accumulate large carbon stores (Griffiths and Harrison, 2009), may continue to synthesize functional biomass in the dark, albeit at a reduced rate (Table 2, Fig. 8).

Our results may have implications for understanding the distribution of very small phytoplankton cells in different oceanic regimes. For example, in environments with deep convection, cells are regularly mixed well below the euphotic depth (Backhaus et al., 1999). Such environments therefore involve prolonged exposure to darkness, and may favor relatively large cells with sufficient capacity for storage. It has been suggested previously that dominance of larger organisms in more variable environments may be linked to the capacity to store nutrients such as phosphorus and iron (Grover, 1991a, 1991b, 2011, Tozzi et al., 2004). The link between cell size, carbon quota, and infrequent PFD has received far less attention.

The prediction that the smallest prokaryotic autotrophs should have a dimished capacity for storage is unsurprising in light of the strong evolutionary pressure toward small cell size in low nutrient environments, which may also have caused *Prochlorococcus* to shrink its genome (Partensky and Garczarek, 2010). *Prochlorococcus* are typically most dominant in relatively stable environments, with very low nutrient supply rates (Partensky et al., 1999). Pressure to optimize nutrient uptake in stable, low nutrient environments is likely to subordinate storage requirements, even when photon

BGD
11, 5179–5214, 2014

supply is intermittent (Fig. 9b and d). Larger organisms tend to dominate in environments with relatively high nutrient input, where small cells are intensely grazed and the need to optimize surface area to volume ratios disappears (Chisholm, 1992; Ward et al., 2013). Our model indicates one additional benefit to large cell size in eutrophic ecosystems.

At high lattitude phytoplankton may be exposed to many months of darkness during winter. Without going into resting stages, tolerance of prolonged exposure to darkness is influenced by the capacity for basal respiration, which is also likely to depend on reserve carbon availability (Furusato and Asaeda, 2009). Organisms able to survive prolonged exposure to darkness without going into resting stage may respond faster when favorable conditions return. Thus, while this work has focused on the benefit of carbon storage to organism growth rates, there may also be ecologically significant benefits to *survival* associated with flexibility in C : N ratio, and accumulation of carbon reserves.

Not all experimental data used to constrain and interpret our model were of organisms in similar culture conditions. For example, while Sakshaug et al. (1989) cultured *S. costatum* over a range of day lengths, Moore et al. (1995) grew *P. marinus* on 14 : 10 light-dark cycles. Furthermore, the C : N data of Bertilsson et al. (2003) were of cyanobacteria in batch culture, exposed to P starvation, which may underestimate the nitrogen starved C : N ratio (Goldman et al., 1979). In addition, none of the data were explicitly of carbohydrate or lipid abundance, and C : N variability was used to infer changes in macromolecular composition. Additional experimental data to further advance the theory presented here include measurements of the accumulation and consumption of different storage carbohydrates and lipids, under conditions of intermittent photon supply for a range of species cultured under comparable experimental conditions.

We did not include a size dependence of the inorganic reserve N quota. By comparison to carbon, phytoplankton typically do not have large quotas for inorganic N; most of the nitrogen "stored" by large phytoplankton is usually proteinacious (Geider

BGD
11, 5179–5214, 2014

and La Roche, 2002). High protein quota may buffer protein degradation, prolonging survival at the individual level. Recycling of nitrogen and carbon contained in proteins may also lead to a more flexible metabolic strategy. Nonetheless, this recycling does not lead to a net gain in the cells' nitrogen or carbon quota. In contrast, carbohydrates, lipids and inorganic forms of N have no direct metabolic function. Their subsequent assimilation into proteins must lead to a net gain in at least one additional elemental quota.

Accumulation of carbon reserves under PFD fluctuations and nutrient limitation have been widely reported (Handa, 1969; Packer et al., 2011), but the ecological significance of this storage is not well understood. Accumulation of storage compounds is nonetheless responsible for large fluctuations in the C : N ratio, so is intimately connected with ocean biogeochemical cycles. Predator–prey interactions are thought to be modulated by cell stoichiometry (Mitra, 2006), so C : N dynamics described here may also influence foodweb interactions.

5 Conclusions

Larger phytoplankton cells able to accumulate a significant amount of reserve carbon polymers may be able to maintain active metabolism in the dark, thereby buffering the effects of prolonged light limitation. While the smallest autotrophs are optimized for nutrient acquisition in oligotrophic environments, they may be less equiped to cope with light limitation often found at high lattitude (Fig. 1). We suggest this is one additional factor that influences the distribution of small and large organisms in different trophic regimes. Furthermore, due to accumulation of carbon storage compounds, large organisms may have a higher potential C : N ratio, and are likely to exhibit a wider range of values. We hope that in future, the model presented may be combined with more detailed descriptions of PFD variability and interspecific interactions, to better understand the influence of carbon storage on large scale patterns of the C : N ratio, and the distributions of different phytoplankton size classes.

BGD
11, 5179–5214, 2014

Acknowledgements. We thank Zoe Finkel for useful comments on previous versions of this manuscript.

References

Anning, T., MacIntyre, H., Pratt, S., Sammes, P., Gibb, S., and Geider, R.: Photoacclimation in the marine diatom *Skeletonema costatum*, Limnol. Oceanogr., 45, 1807–1817, doi:10.4319/lo.2000.45.8.1807, 2000. 5208

Armstrong, R.: Grazing limitation and nutrient limitation in marine ecosystems: steady state solutions of an ecosystem model with multiple food chains, Limnol. Oceanogr., 39, 597–608, doi:10.4319/lo.1994.39.3.0597, 1994. 5180

Armstrong, R.: Optimality-based modeling of nitrogen allocation and photoacclimation in photosynthesis, Deep-Sea Res. Pt. II, 53, 513–531, doi:10.1016/j.dsr2.2006.01.020, 2006. 5185

Backhaus, J., Wehde, H., Hegseth, E., and Kämpf, J.: "Phyto-convection": the role of oceanic convection in primary production, Mar. Ecol.-Prog. Ser., 189, 77–92, doi:10.3354/meps189077, 1999. 5193

Bertilsson, S., Berglund, O., Karl, D., and Chisholm, S.: Elemental composition of marine *Prochlorococcus* and *Synechococcus*: implications for the ecological stoichiometry of the sea, Limnol. Oceanogr., 48, 1721–1731, doi:10.4319/lo.2003.48.5.1721, 2003. 5189, 5194, 5211

Blackford, J., Allen, J., and Gilbert, F.: Ecosystem dynamics at six contrasting sites: a generic modelling study, J. Marine Syst., 52, 191–215, doi:10.1016/j.jmarsys.2004.02.004, 2004. 5180

Borghans, J., De Boer, R., and Segel, L.: Extending the quasi-steady state approximation by changing variables, B. Math. Biol., 58, 43–63, doi:10.1007/BF02458281, 1996. 5185

Brewin, R., Sathyendranath, S., Hirata, T., Lavender, S., Barciela, R., and Hardman-Mountford, N.: A three-component model of phytoplankton size class for the Atlantic Ocean, Ecol. Model., 221, 1472–1483, doi:10.1016/j.ecolmodel.2010.02.014, 2010. 5180

Caperon, J. and Meyer, J.: Nitrogen-limited growth of marine phytoplankton – I. Changes in population characteristics with steady-state growth rate, Deep-Sea Res., 19, 601–618, doi:10.1016/0011-7471(72)90089-7, 1972. 5187

BGD
11, 5179–5214, 2014

Chisholm, S. W.: Phytoplankton size, Primary productivity and biogeochemical cycles in the sea, Plenum, 213–237, doi:10.1007/978-1-4899-0762-2_12, 1992. 5180, 5181, 5194
Clark, J., Daines, S., Williams, H., and Lenton, T.: Environmental selection and resource allocation determine spatial patterns in picophytoplankton cell size, Limnol. Oceanogr., 58, 1008–1022, 2013. 5181
de Boyer Montegut, C., Madec, G., Fischer, A. S., Lazar, A., and Iudicone, D.: Mixed layer depth over the global ocean: an examination of profile data and a profile-based climatology, J. Geophys. Res.-Oceans, 109, C12003, doi:10.1029/2004JC002378, 2004. 5206
DiTullio, G. and Laws, E.: Diel periodicity of nitrogen and carbon assimilation in five species of marine phytoplankton: accuracy of methodology for predicting N-assimilation rates and N/C composition ratios, Mar. Ecol.-Prog. Ser., 32, 123–132, 1986. 5185, 5190, 5202, 5203
Dortch, Q., Clayton Jr, J., Thoresen, S., and Ahmed, S.: Species differences in accumulation of nitrogen pools in phytoplankton, Mar. Biol., 81, 237–250, doi:10.1007/BF00393218, 1984. 5188
Droop, M.: Nutrient limitation in osmotrophic protista, Am. Zool., 13, 209–214, doi:10.1093/icb/13.1.209, 1973. 5187
Dubinsky, Z. and Schofield, O.: From the light to the darkness: thriving at the light extremes in the oceans, Hydrobiologia, 639, 153–171, doi:10.1007/s10750-009-0026-0, 2010. 5181
Edwards, E., Mridul, T., Klausmeier, K., and Litchman, E.: Light and growth in marine phytoplankton: allometric, taxanomic, and environmental variation, in preparation, 2014. 5187
Falkowski, P. and Raven, J.: Aquatic Photosynthesis, Princeton University Press, 2007. 5202
Furusato, E. and Asaeda, T.: A dynamic model of darkness tolerance for phytoplankton: model description, Hydrobiologia, 619, 67–88, doi:10.1007/s10750-008-9601-z, 2009. 5194
Geider, R. and La Roche, J.: Redfield revisited: variability in the C : N : P of phytoplankton and its biochemical basis, Eur. J. Phycol., 37, 1–17, doi:10.1017/S0967026201003456, 2002. 5194, 5195, 5202
Geider, R., MacIntyre, H., and Kana, T.: Dynamic model of phytoplankton growth and acclimation: responses of the balanced growth rate and the chlorophyll a: carbon ratio to light, nutrient-limitation and temperature, Mar. Ecol.-Prog. Ser., 148, 187–200, doi:10.3354/meps148187, 1997. 5185
Geider, R., MacIntyre, H., and Kana, T.: A dynamic regulatory model of phytoplanktonic acclimation to light, nutrients, and temperature, Limnol. Oceanogr., 43, 679–694, doi:10.4319/lo.1998.43.4.0679, 1998. 5185, 5202

BGD
11, 5179–5214, 2014

Goldman, J., McCarthy, J., and Peavey, D.: Growth rate influence on the chemical composition of phytoplankton in oceanic waters, Nature, 279, 210–215, doi:10.1038/279210a0, 1979. 5194

Granum, E., Kirkvold, S., and Myklestad, S.: Cellular and extracellular production of carbohydrates and amino acids by the marine diatom Skeletonema costatum: diel variations and effects of N depletion, Mar. Ecol.-Prog. Ser., 242, 83–94, doi:10.3354/meps242083, 2002. 5181

Griffiths, M. and Harrison, S.: Lipid productivity as a key characteristic for choosing algal species for biodiesel production, J. Appl. Phycol., 21, 493–507, doi:10.1007/s10811-008-9392-7, 2009. 5193

Grover, J.: Resource competition in a variable environment: phytoplankton growing according to the variable-internal-stores model, Am. Nat., 138, 811–835, doi:10.1086/285254, 1991a. 5181, 5193

Grover, J. P.: Dynamics of competition among microalgae in variable environments: experimental tests of alternative models, Oikos, 62, 231–243, doi:10.2307/3545269, 1991b. 5181, 5193

Grover, J.: Resource storage and competition with spatial and temporal variation in resource availability, Am. Nat., 178, E124–E148, doi:10.1086/662163, 2011. 5181, 5193

Hama, T.: Production and turnover rates of fatty acids in marine particulate matter through phytoplankton photosynthesis, Mar. Chem., 33, 213–227, doi:10.1016/0304-4203(91)90068-8, 1991. 5202

Handa, N.: Carbohydrate metabolism in the marine diatom Skeletonema costatum, Mar. Biol., 4, 208–214, doi:10.1007/BF00393894, 1969. 5195

Healey, F.: Interacting effects of light and nutrient limitation on the growth rate of *Synechococcus linearis* (cyanophecae)[1], J. Phycol., 21, 134–146, doi:10.1111/j.0022-3646.1985.00134.x, 1985. 5189, 5211

Hirata, T., Aiken, J., Hardman-Mountford, N., Smyth, T., and Barlow, R.: An absorption model to determine phytoplankton size classes from satellite ocean colour, Remote Sens. Environ., 112, 3153–3159, doi:10.1016/j.rse.2008.03.011, 2008. 5180

Kameda, T. and Ishizaka, J.: Size-fractionated primary production estimated by a two-phytoplankton community model applicable to ocean color remote sensing, J. Oceanogr., 61, 663–672, doi:10.1016/j.rse.2008.03.011, 2005. 5180

BGD
11, 5179–5214, 2014

Le Quéré, C., Harrison, S. P., Prentice, C., Buitenhuis, E. T., Aumont, O., Bopp, L., Claustre, H., Cotrim Da Cunha, L., Geider, R. J., Giraud, X., Klaas, C., Kohfeld, K. E., Legendre, L., Manizza, M., Platt, T., Rivkin, R. B., Sathyendranath, S., Uitz, J., Watson, A. J., and Wolf-Gladrow, D.: Ecosystem dynamics based on plankton functional types for global ocean biogeochemistry models, Glob. Change Biol., 11, 2016–2040, doi:10.1111/j.1365-2486.2005.1004.x, 2005. 5180

Litchman, E., Klausmeier, C., Schofield, O., and Falkowski, P.: The role of functional traits and trade-offs in structuring phytoplankton communities: scaling from cellular to ecosystem level, Ecol. Lett., 10, 1170–1181, doi:10.1111/j.1461-0248.2007.01117.x, 2007. 5202, 5204

Lourenço, S., Barbarino, E., Marquez, U., and Aidar, E.: Distribution of intracellular nitrogen in marine microalgae: basis for the calculation of specific nitrogen-to-protein conversion factors, J. Phycol., 34, 798–811, 1998. 5188, 5202

McKew, B., Davey, P., Finch, S., Hopkins, J., Lefebvre, S., Metodiev, M., Oxborough, K., Raines, C., Lawson, T., and Geider, R.: The trade-off between the light-harvesting and photoprotective functions of fucoxanthin-chlorophyll proteins dominates light acclimation in Emiliania huxleyi (clone CCMP 1516), New Phytol., 200, 74–85, doi:10.1111/nph.12373, 2013. 5183, 5185

Mei, Z.-P., Finkel, Z., and Irwin, A.: Phytoplankton growth allometry and size dependent C : N stoichiometry revealed by a variable quota model, Mar. Ecol.-Prog. Ser., 434, 29–43, doi:10.3354/meps09149, 2011. 5188, 5204

Menden-Deuer, S. and Lessard, E.: Carbon to volume relationships for dinoflagellates, diatoms, and other protist plankton, Limnol. Oceanogr., 45, 569–579, doi:10.4319/lo.2000.45.3.0569, 2000. 5189, 5204

Mitra, A.: A multi-nutrient model for the description of stoichiometric modulation of predation in micro-and mesozooplankton, J. Plankton Res., 28, 597–611, doi:10.1093/plankt/fbi144, 2006. 5195

Moore, L., Goericke, R., and Chisholm, S.: Comparative physiology of *Synechococcus* and *Prochlorococcus*: influence of light and temperature on growth, pigments, fluorescence and absorptive properties, Mar. Ecol.-Prog. Ser., 116, 259–275, doi:10.3354/meps116259, 1995. 5189, 5194, 5210

Morel, A. and Bricaud, A.: Theoretical results concerning light absorption in a discrete medium, and application to specific absorption of phytoplankton, Deep-Sea Res., 28, 1375–1393, doi:10.1016/0198-0149(81)90039-X, 1981. 5181, 5186, 5202

BGD
11, 5179–5214, 2014

Packer, A., Li, Y., Andersen, T., Hu, Q., Kuang, Y., and Sommerfeld, M.: Growth and neutral lipid synthesis in green microalgae: a mathematical model, Bioresource Technol., 102, 111–117, doi:10.1016/j.biortech.2010.06.029, 2011. 5195

Pahlow, M.: Linking chlorophyll-nutrient dynamics to the Redfield N : C ratio with a model of optimal phytoplankton growth, Mar. Ecol.-Prog. Ser., 287, 33–43, doi:10.3354/meps287033, 2005. 5202

Partensky, F. and Garczarek, L.: *Prochlorococcus:* advantages and limits of minimalism, Annu. Rev. Mar. Sci., 2, 305–331, doi:10.1146/annurev-marine-120308-081034, 2010. 5193

Partensky, F., Hess, W., and Vaulot, D.: *Prochlorococcus*, a marine photosynthetic prokaryote of global significance, Microbiol. Mol. Biol. R., 63, 106–127, 1999. 5193

Pasciak, W. and Gavis, J.: Transport limitation of nutrient uptake in phytoplankton, Limnol. Oceanogr., 19, 881–888, doi:10.4319/lo.1974.19.6.0881, 1974. 5180

Probyn, T., Waldron, H., Searson, S., and Owens, N.: Diel variability in nitrogenous nutrient uptake at photic and subphotic depths, J. Plankton Res., 18, 2063–2079, doi:10.1093/plankt/18.11.2063, 1996. 5185

Rodolfi, L., Chini Zittelli, G., Bassi, N., Padovani, G., Biondi, N., Bonini, G., and Tredici, M.: Microalgae for oil: strain selection, induction of lipid synthesis and outdoor mass cultivation in a low-cost photobioreactor, Biotechnol. Bioeng., 102, 100–112, doi:10.1002/bit.22033, 2009. 5189, 5191, 5192

Ross, O. and Geider, R.: New cell-based model of photosynthesis and photo-acclimation: accumulation and mobilisation of energy reserves in phytoplankton, Mar. Ecol.-Prog. Ser., 383, 53–71, doi:10.3354/meps07961, 2009. 5185

Sakshaug, E., Andresen, K., and Kiefer, D.: A steady state description of growth and light absorption in the marine planktonic diatom *Skeletonema costatum*, Limnol. Oceanogr., 34, 198–205, doi:10.4319/lo.1989.34.1.0198, 1989. 5189, 5194, 5211, 5212

Shuter, B.: Size dependence of phosphorus and nitrogen subsistence quotas in unicellular microorganisms [Cyanophyta and other Algae species]., Limnol. Oceanogr., 23, 1248–1255, doi:10.4319/lo.1978.23.6.1248, 1978. 5188

Tang, E.: The allometry of algal growth rates, J. Plankton Res., 17, 1325–1335, doi:10.1093/plankt/17.6.1325, 1995. 5180

Thingstad, T.: Utilization of N, P, and organic C by heterotrophic bacteria. I. Outline of a chemostat theory with a consistent concept of maintenance metabolism, Mar. Ecol.-Prog. Ser., 35, 99–100, doi:10.3354/meps035099, 1987. 5184

BGD
11, 5179–5214, 2014

Tozzi, S., Schofield, O., and Falkowski, P.: Historical climate change and ocean turbulence as selective agents for two key phytoplankton functional groups, Mar. Ecol.-Prog. Ser., 274, 123–132, doi:10.3354/meps274123, 2004. 5181, 5193

Uitz, J., Huot, Y., Bruyant, F., Babin, F., and Claustre, H.: Relating phytoplankton photophysiological properties to community structure on large scales, Limnol. Oceanogr., 52, 614–630, doi:10.4319/lo.2008.53.2.0614, 2008. 5180

Verdy, A., Follows, M., and Flierl, G.: Optimal phytoplankton cell size in an allometric model, Mar. Ecol.-Prog. Ser., 379, 1–12, doi:10.3354/meps07909, 2009. 5181, 5188

Ward, B., Dutkiewicz, S., Jahn, O., and Follows, M.: A size-structured food-web model for the global ocean, Limnol. Oceanogr., 57, 1877, doi:10.4319/lo.2012.57.6.1877, 2012. 5181

Ward, B., Dutkiewicz, S., and Follows, M.: Modelling spatial and temporal patterns in marine plankton communities: top-down and bottom-up controls, J. Plankton Res., 36, 31–47, doi:10.1093/plankt/fbt097, 2013. 5194

BGD
11, 5179–5214, 2014

Table 1. Parameters and variables with associated units. Where appropriate values were found in the literature, the source is indicated. The half saturations for biosynthesis, K_C and K_N, were assumed here to be small, representing high turnover of internal reserves (e.g. Hama, 1991). Note that the units of V_{max} were obtained by dividing the units reported by Litchman et al. (2007) by their units for Q^N_{min} (see also Table 3).

Symbol	Description	Value	Units	Source
C_R	reserve carbon	variable	$mmol\,C\,m^{-3}$	–
C_F	functional carbon	variable	$mmol\,C\,m^{-3}$	–
N_R	reserve nitrogen	variable	$mmol\,N\,m^{-3}$	–
N_F	functional nitrogen	variable	$mmol\,N\,m^{-3}$	–
S	substrate concentration	variable	$\mu mol\,L^{-1}$	–
E	photon flux density (PFD)	variable	$mol\ photons\ m^{-2}\,day^{-1}$	–
V_n	nitrogen uptake rate	variable	day^{-1}	–
V_m	maximum nitrogen uptake at N_R	variable	day^{-1}	–
V_{max}	maximum nitrogen uptake rate	allometric	day^{-1}	Litchman et al. (2007)
K_S	nitrogen uptake half saturation	allometric	$\mu mol\,L^{-1}$	Litchman et al. (2007)
P_n	carbon fixation rate	variable	$mmol\,C\,(mmol\,N)^{-1}\,day^{-1}$	–
P_m	carbon fixation rate at C_R	variable	$mmol\,C\,(mmol\,N)^{-1}\,day^{-1}$	–
P_{max}	maximum carbon fixation rate	see Table 4	$mmol\,C\,(mmol\,N)^{-1}\,day^{-1}$	–
a_{ph}	light absorption	allometric	$m^2\,(mol\,N)^{-1}$	Morel and Bricaud (1981)
a^*_{ph}	light absorption in solution	490.0	$m^2\,(mol\,N)^{-1}$	–
ϕ_m	maximum quantum efficiency	0.08	$mol\,C\,(mol\,photons)^{-1}$	Falkowski and Raven (2007)
γ	taxanomic initial slope factor	see Table 4	–	–
F_{LH}	fraction of cellular nitrogen allocated to light harvesting	variable	–	–
ρ_{LH}	fraction of cellular nitrogen allocated to synthesis of light harvesting apparatus	variable	–	–
F^{max}_{LH}	maximum nitrogen allocation to light harvesting	see Table 4	–	–
F^{min}_{LH}	maximum nitrogen allocation to light harvesting	see Table 4	–	–
F^G_{LH}	curvature of allocation to light harvesting	see Table 4	$m^2\,day\,mol\,photon\,s^{-1}$	–
θ_N	Chl : N of light harvesting apparatus	2.4	$g\,Chl\,g\,N^{-1}$	–
N^{max}_R	maximum reserve nitrogen	variable	$mmol\,N\,m^{-3}$	–
C^{max}_R	maximum reserve carbon	variable	$mmol\,C\,m^{-3}$	–
f_{stor}	maximum reserve nitrogen as fraction of functional pool	0.2	–	Lourenço et al. (1998)
K_C	carbon reserve half saturation coefficient	0.01	–	–
K_N	nitrogen reserve half saturation coefficient	0.01	–	–
μ_{max}	maximum biosynthesis rate	see Table 4	day^{-1}	–
ζ	cost of biosynthesis	3.0	$mmol\,C\,(mmol\,N)^{-1}$	Pahlow (2005)
η	N : C ratio of functional components	0.17	$mmol\,N\,(mmol\,C)^{-1}$	Geider and La Roche (2002)
R_0	maintenance respiration	0.01	$mmol\,C\,(mmol\,N)^{-1}\,day^{-1}$	Geider et al. (1998)
a_N	reduction in dark N assimilation	0.59	–	DiTullio and Laws (1986)
V	individual cell volume	see Table 3	μm^3	–

BGD
11, 5179–5214, 2014

Table 2. Diurnal changes in nitrogen assimilation based on ^{14}C incorporated into proteins. Data are from DiTullio and Laws (1986). Data are given as percentage of total N assimilation calculated with CHN analyses (DiTullio and Laws, 1986). Average reduction in dark N assimilation (i.e. a_N) is 0.59.

Species	light (12 h)	dark (12 h)	ratio
P. tricornutum (diatom)	101	74	0.73
P. lutheri (prymnesiophyceae)	98	79	0.81
Isochrysis sp. (dinoflagellate)	154	95	0.62
A. carteri (dinoflagallate)	213	40	0.19
D. salina (halophile)	119	70	0.59

BGD
11, 5179–5214, 2014

Table 3. Allometric parameters for power law functions of the form aV^b. Note that the values for V_{max} were converted from Litchman et al. (2007) by dividing through by their relationship for Q^N_{min}. The specific values were calculated assuming spherical cells with diameters 0.6, 1.5 and 10.0 for *P. marinus*, *Synechococcus* and *S. costatum* respectively.

Symbol	Units	a	b	Source
V_{max}	day^{-1}	6.69	−0.1	Litchman et al. (2007)
K_S	$\mu mol\,L^{-1}$	0.17	0.27	Litchman et al. (2007)
Q^C_{max}	$mmol\,C\,cell^{-1}$	18×10^{-12}	0.9	Menden-Deuer and Lessard (2000)
$Q^C_{F,min}$	$mmol\,C\,cell^{-1}$	9.9×10^{-12}	0.72	Mei et al. (2011)

BGD
11, 5179–5214, 2014

Table 4. Species specific parameter values.

	P. marinus (MED4)	*P. marinus* (SS120)	*Synechococcus* (WH8103)	*Synechococcus* (WH8012)	*S. linearis*	*Skeletonema costatum*
P_{max}	18.0	18.0	18.0	18.0	18.0	18.0
F_{LH}^{max}	0.14	0.14	0.06	0.06	0.06	0.15
F_{LH}^{min}	0.0375	0.0375	0.033	0.033	0.033	0.033
F_{LH}^{G}	0.3	0.3	0.07	0.07	0.07	0.14
μ_{max}	0.6	0.6	0.65	1.5	1.3	1.5
γ	1.0	1.0	1.0	1.0	1.0	2.0

BGD
11, 5179–5214, 2014

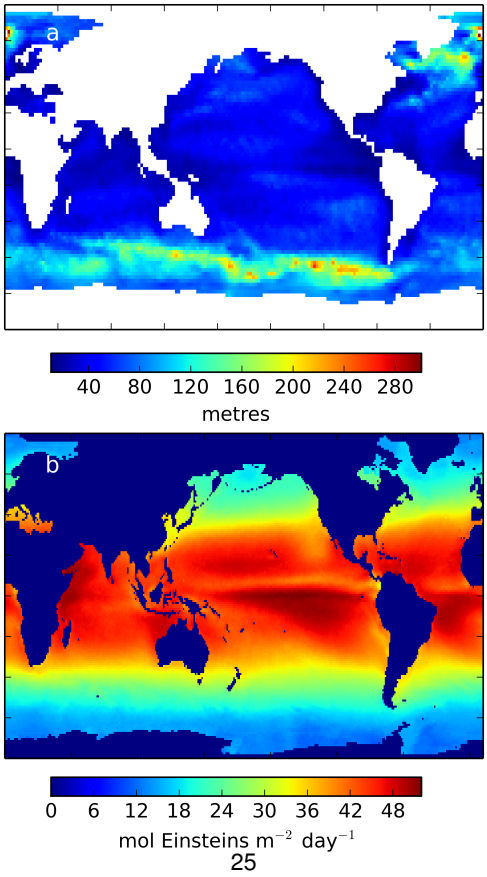

25

Fig. 1. Global average mixed layer depth (MLD, panel **a**) and surface photon flux density (PFD) **(b)**. Climatology of MLD is from de Boyer Montegut et al. (2004) and surface PFD is from SeaWiFS. At high lattitude there is on average deeper mixing and low surface PFD, which may be limiting to phytoplankton growth.

BGD
11, 5179–5214, 2014

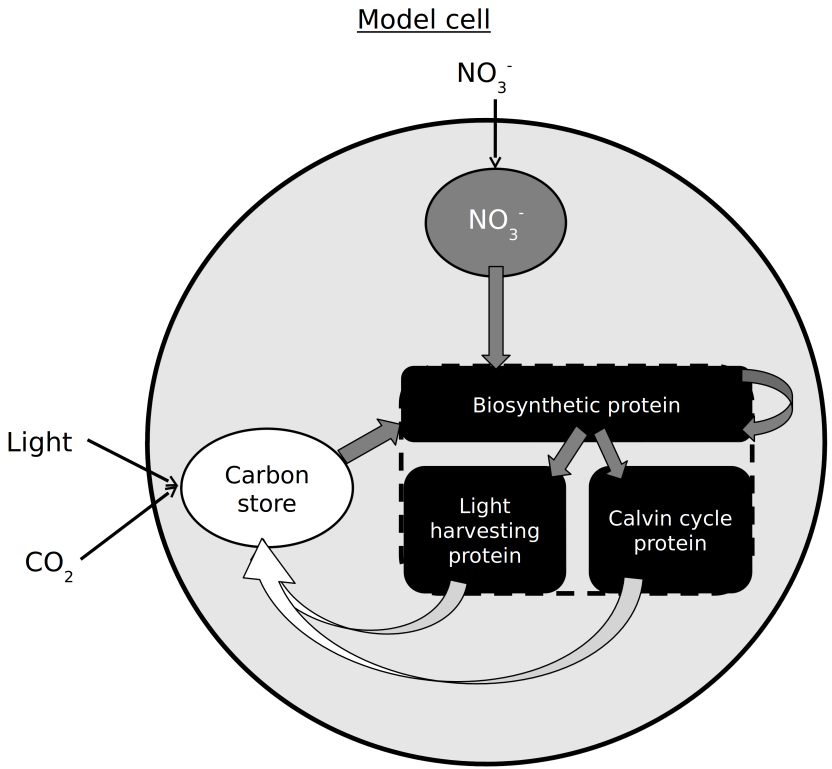

Fig. 2. Schematic representation of the phytoplankton growth model. Light and CO_2 enter the carbon store via photosynthesis, whereas inorganic forms of nitrogen (assumed here to be NO_3^-) are passed through transport proteins in the cell's plasma membrane. Carbon and nitrogen in the reserve pools is converted to functional apparatus via the cell's biosynthetic machinery. The functional apparatus contains proteins involved in photosynthesis and biosynthesis, and contains carbon and nitrogen in a ratio that is assumed here to be constant.

BGD
11, 5179–5214, 2014

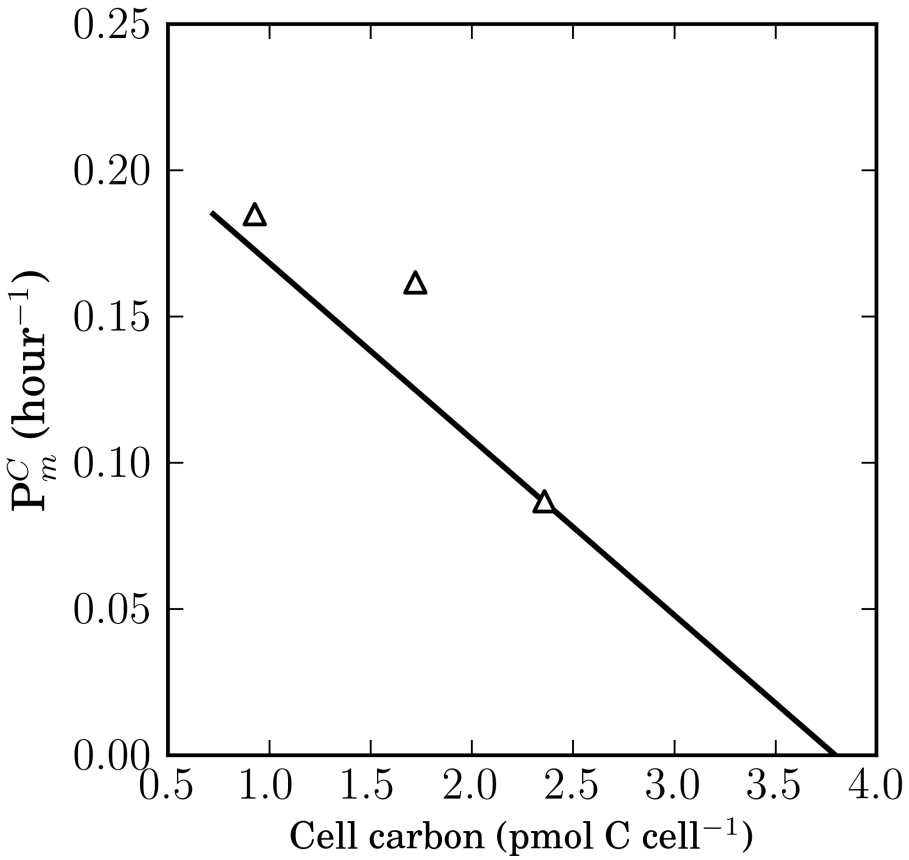

Fig. 3. Regulation of P_m^C in the diatom *Skeletonema costatum* (data from Anning et al., 2000). The triangles are experimental observations, the solid black line is Eq. (8) converted to carbon units with $P_m^C = \eta P_m/24$ and $P_{max} = 29.6$

BGD
11, 5179–5214, 2014

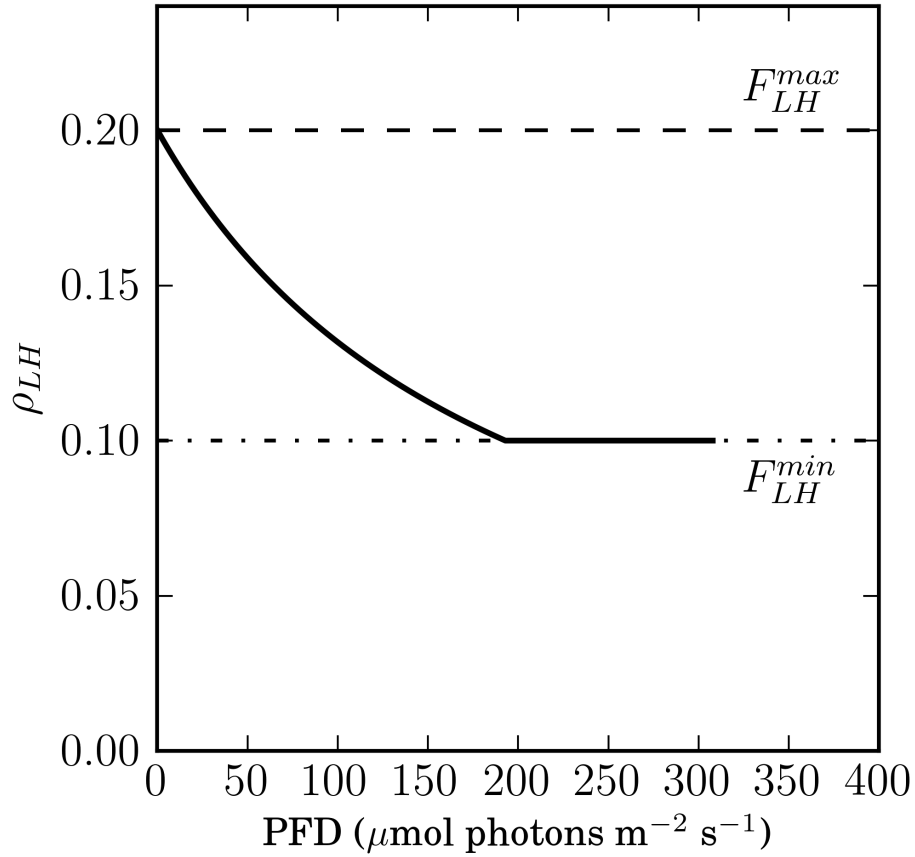

Fig. 4. Demonstration of the modeled regulation of nitrogen allocation to light harvesting with Eq. (9). There is a non-linear reduction in light harvesting apparatus as a function of PFD (see also Fig. 5). Parameters for this figure: $F_{\mathrm{LH}}^{\mathrm{min}} = 0.1$, $F_{\mathrm{LH}}^{\mathrm{max}} = 0.2$ and $F_{\mathrm{LH}}^{G} = 0.06$.

BGD
11, 5179–5214, 2014

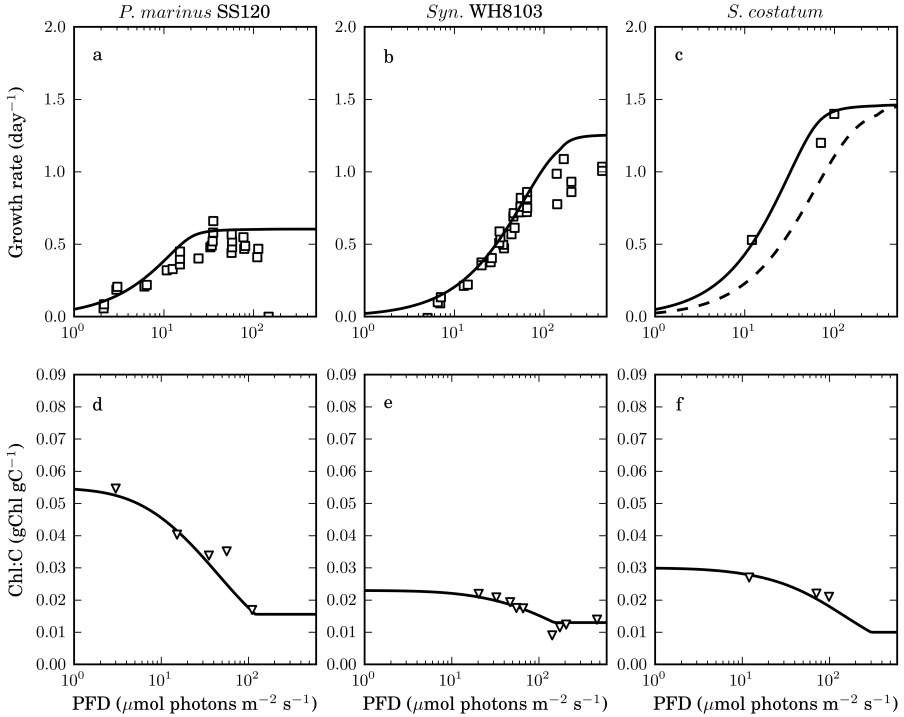

Fig. 5. Model-data comparison for growth rates and Chl : C ratios under PFD limited, balanced growth conditions. Parameters in Table 4 were manually tuned to yeild a close fit. In all cases, black lines are model predictions; open squares and triangles correspond to measured growth and Chl : C ratios. Model predictions of the fraction of cellular nitrogen allocated to light harvesting were converted to the units in **(d–f)** with Chl : C = $F_{LH}\eta\theta_N$, where θ_N is the Chl : N of the light harvesting apparatus (Table 1). The dashed line in **(c)** is the modeled growth-irradiance curve if the tuning parameter γ were not applied. Note that the Chl cell^{-1} measurements of Moore et al. (1995) were converted to Chl : C ratios by dividing through by the size specific Q^C_{max} (Table 3).

BGD
11, 5179–5214, 2014

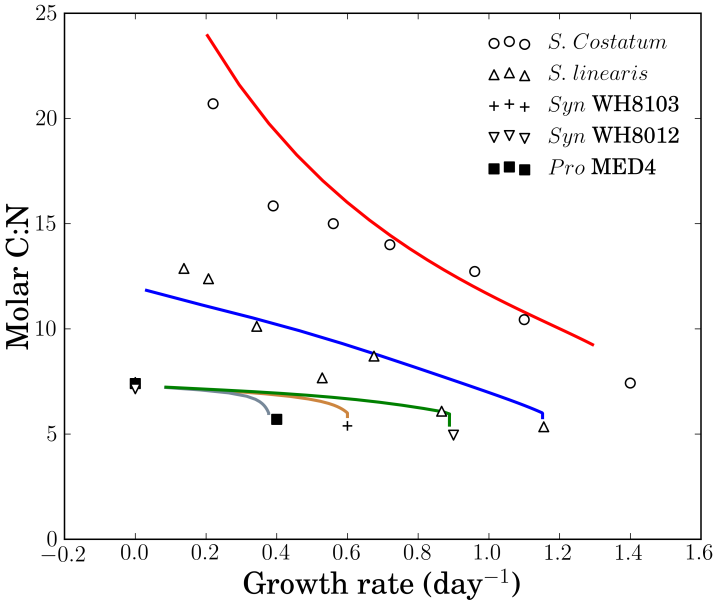

Fig. 6. Model-data comparison of whole cell C : N ratio under conditions of nutrient limited, balanced growth. In all cases, the C : N ratio increases as nutrient supply diminishes. *S. costatum* (Sakshaug et al., 1989) have a higher C : N ratio by comparison to *S. linearis* (Healey, 1985) and other cyanobacteria (Bertilsson et al., 2003) at very low growth rates. The red, blue and green lines are model predictions for cell sizes corresponding to *S. costatum*, *S. linearis* and WH8012 respectively. Gray and brown lines are model predictions of *Prochlorococcus* MED4 and *Synechococcus* WH8103. Modeled PFD matched the experimental conditions which were 30–40 µmol photons m^{-2} s^{-1} for MED4, WH8012, WH8103; 80 µmol photons m^{-2} s^{-1} for *S. linearis* and 1200 µmol photons m^{-2} s^{-1} for *S. costatum*. *S. linearis* and *S. costatum* were N limited in chemostats, whereas MED4, WH8012 and WH8103 were P limited in batch culture. These data may be less than the nitrogen limited C : N if, for example, P limited organisms are still able to accumlate inorganic N.

BGD
11, 5179–5214, 2014

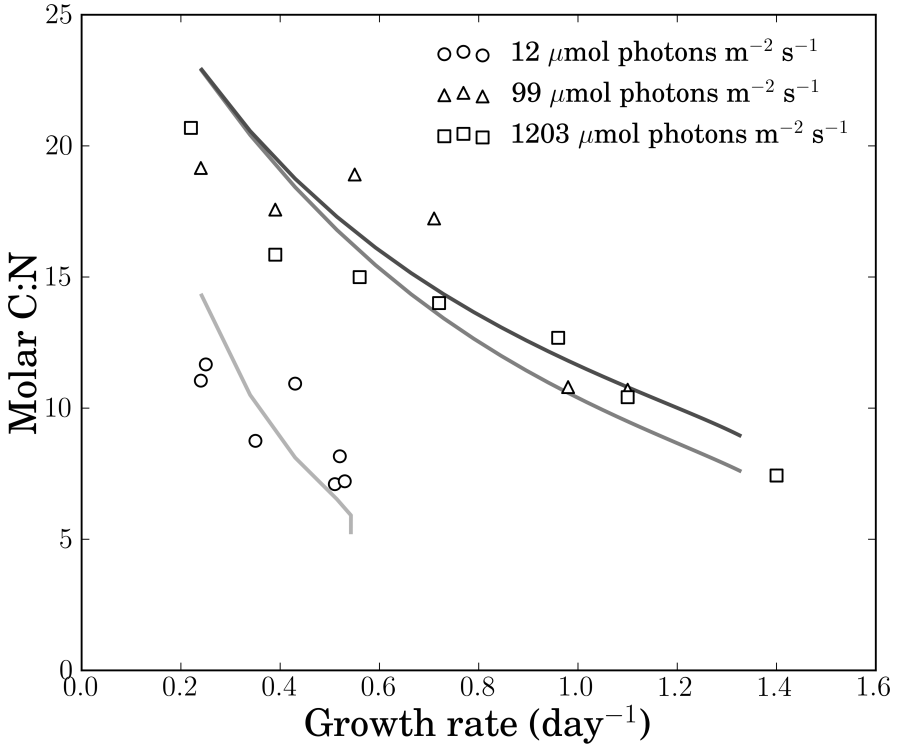

Fig. 7. Dependence of C : N on nitrogen limited growth rate for the diatom *S. costatum* cultured under a range of light intensities (Sakshaug et al., 1989). Symbols are experimental measurements, and gray lines are model results. The modeled light conditions matched the experimental conditions. Even when grown under extremely low PFD, *S. costatum* has a much wider range in C : N than the oceanic cyanobacteria in Fig. 6.

BGD
11, 5179–5214, 2014

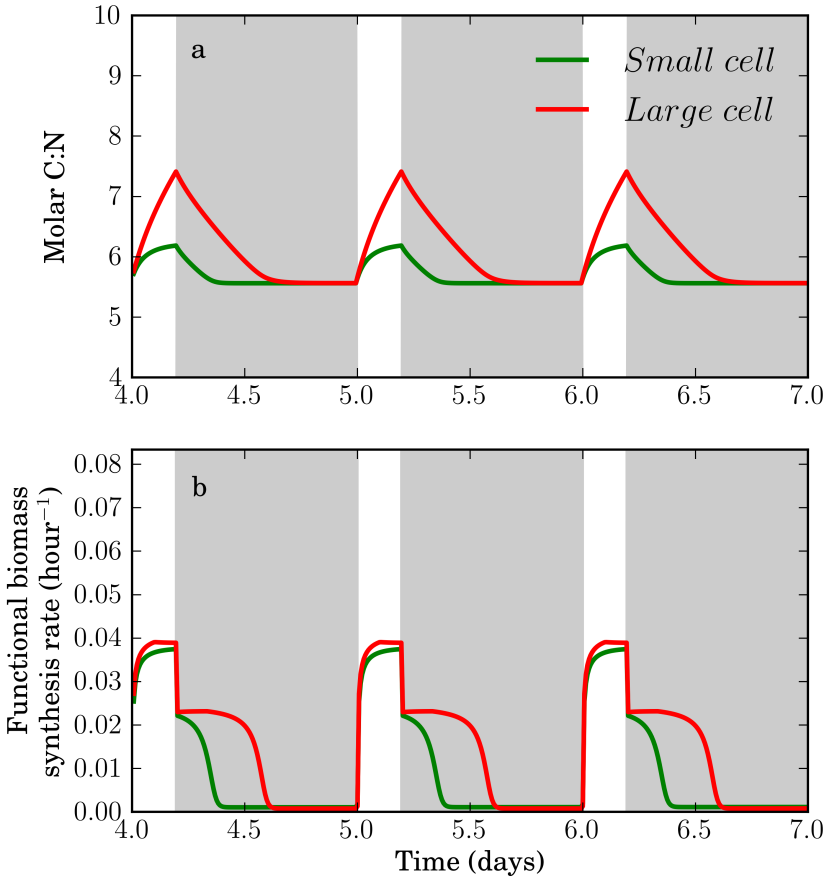

Fig. 8. Model predictions of carbon accumulation and mobilization in two hypothetical organisms of different size. Shaded regions correspond to complete darkness, whereas light regions correspond to 1000 µmol photons m^{-2} s^{-1}. **(a)** Model predictions of variation in cellular C : N ratio. **(b)** Functional biomass synthesis rate determined with Eq. (10).

BGD
11, 5179–5214, 2014

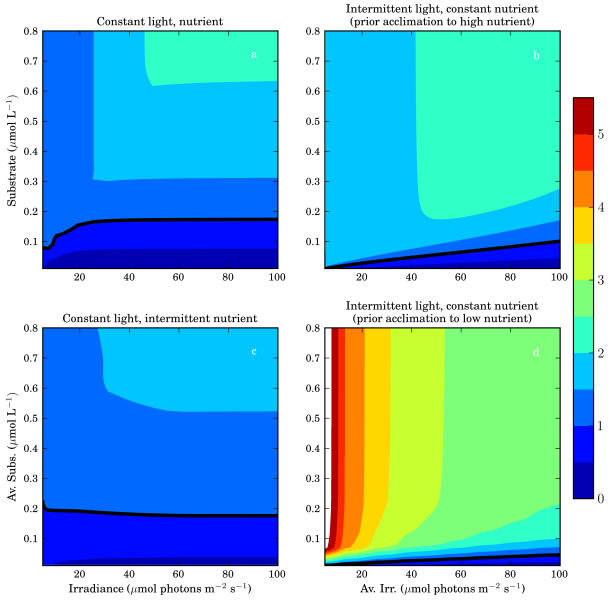

Fig. 9. Contour plots depicting the ratio of *S. costatum* to *P. marinus* (SS120) average daily growth rate in a range of PFD and nutrient conditions. In all cases, ratios of *S. costatum* to SS120 growth rate are contoured over the average, 24 h nitrogen and PFD conditions. Warm colored regions indicate *S. costatum* should have an advantage in terms of average daily growth rate. Cool colored regions corresponding to values less than unity indicate SS120 should grow faster. **(a)** constant light, constant nutrient conditions. Small cells have higher growth rates whenever nitrogen supply is low. **(b)** Constant nutrient; PFD "switched" between 200 µmol photons m^{-2} s^{-1} and complete darkness. When PFD is supplied for very short periods, large cells can grow significantly faster than small cells, because they can store carbon. **(c)** Constant PFD; nitrogen supply "switched" between 1 and 0 µmol photons L^{-1}. **(d)** Same experiment as in panel **(b)**, this time modeled organisms were "acclimated" to low nitrogen concentrations prior to exposure to intermittent PFD. The model was then forced with saturating nitrogen supply for the duration of exposure to intermittent PFD.

BGD
11, 5179–5214, 2014